POTENTIAL FLOW BASED OPTIMIZATION OF A HIGH SPEED, FOIL-ASSISTED, SEMI-PLANNING CATAMARAN FOR LOW WAKE

Daniele Peri[1], Emilio F. Campana[1], Manivannan Kandasamy[2], Seng Keat Ooi[2], Pablo Carrica[2], Fred Stern[2], Phil Osborne[3], Neil Macdonald[4], Nic de Waal[5]

[1] INSEAN, The Italian Ship Model Basin, Rome, Italy

[2] IIHR-Hydroscience & Engineering, The University of Iowa, Iowa, USA

[3] Golder Associates Incorporated, USA

[4] Coldwater Consulting Ltd.

[5] Teknicraft Design Ltd.

ABSTRACT

In this paper, a sensitivity analysis and the numerical optimization of an initial design for a fast foil-assisted catamaran ferry are described, with the goal of both reducing wakes and increasing fuel efficiency. The procedure is split into two phases: 1. Starting from an initial design, a set of new hull shapes was automatically generated and evaluated, via a potential flow solver. These results were successively used to derive information about the influence of each design parameter. 2. A multi-objective design problem, with 3 objective functions, was formulated and solved and the best trade-off solutions (belonging to the *Pareto* optimal set) were identified. The potential flow optimization lead to a new hull geometry that was optimized in terms of bow shape, foil thickness, foil position, and demi-hull spacing providing a basis for improvements by the naval architect and the starting point for a more detailed optimization with a RANS solver.

1. INTRODUCTION

The growing complexity of ship's requirements makes the use of heuristic design methods alone increasingly challenging, and there is the awareness that meeting a minimal set of requirements may not suffice to ensure success of new designs. One should, instead, look for optimal designs, with increased reliance on rigorous computational methods. Simulation Based Design (SBD) is an upcoming tool also in the field of ship design: it combines one or more numerical solvers with an optimization scheme and a parameterization tool for shape manipulation, all coordinated into an automatic, non-interactive, framework. SBD automatically provides an optimal design, once a mathematical programming problem in terms of objectives, operative conditions and constraints is formulated. It should be noted that SBD is not and, arguably, will never be push-button design. Rather, it is a suite of approaches that should provide the designer with design alternatives - rapidly generated - while expanding the dimensionality of the design and function spaces: in other words, assisting the designer in exploring the design space more *quickly*, *efficiently*, and *creatively*.

In this paper, an example of the use of this kind of synergy is illustrated. In the design of a passenger only, fast catamaran ferry operating in confined waterways, attention was focused on the waves generated that can potentially cause dangerous impacts to shorelines. At the same time, another request was to increase the fuel efficiency. The problem was tackled with the aid of an SBD framework, by using three different objective functions to drive the final shape selection process. The work started with a preliminary study of a different geometry (SPIRIT) reported in Fig. 1, on which an experimental study was been previously carried out (Osborne et al.,2009). Starting from the hull lines of SPIRIT, a new design (hereafter referred as **RV2**), meeting the requirements of the designer, was finally obtained, and. a first investigation (*PHASE-A*) about the effect of a shape variation of the hull, the foils and of their mutual position was performed. *PHASE-B* involved the complete redesign of the bow and of the foil by using a morphing technique: three base designs were produced by Teknicraft Design Ltd., on the base of the indications coming from the results of the sensitivity study.

The *INSEAN* SBD framework was then applied to solve the constrained multiobjective optimization problem. A set of optimal configurations with respect to three different criteria was finally derived and the final design was eventually identified. Finally a sensitivity analysis around the optimal shape was produced, in order to understand the hydrodynamic qualities of the selected geometry and to give practical, useful indications to the designers.

Fig 1: The demihull of the SPIRIT design.

The SBD framework is based on (1) a free surface, potential flow solver to evaluate the ship performances, (2) a suite of derivative-free, global optimization algorithms capable to solve single and multiobjective constrained optimization problems (Pinto et al, 2007, Campana et al. 2009), and (3) an automatic geometry and mesh modification module. As a prerequisite for the use of an SBD it is of course fundamental to establish the accuracy of the numerical solver adopted for the analysis. The potential flow solver *WARP* (Bassanini et al., 1997) has dynamic heave and trim capabilities. Vorticity shed into the fluid from lifting surfaces is simulated via straight trailing vortices that are assumed leaving the foils (both trailing edge and tip) at unknown angle (Bollay, 1939; Landrini and Campana, 1996). Several tests were performed at both sub- and supercritical speeds. Fine grid computations were performed using 35 panels for each hull length (up to 16000 panels on the free surface) plus 5600 panels on the hull. The grid used in most of the computations is 2200 panels on the hull and 10000 on the free surface. Since the heave and trim effects proved to be fundamental in the comparison with the experiments, a new version of the code was developed to include the effects of the thrust on the equilibrium equations and affect both the power and the heave and trim values. The effect of the thrust was to reduce the predicted power throughout the speed range: the lower Fr numbers becoming less accurate and the high Fr numbers more accurate.

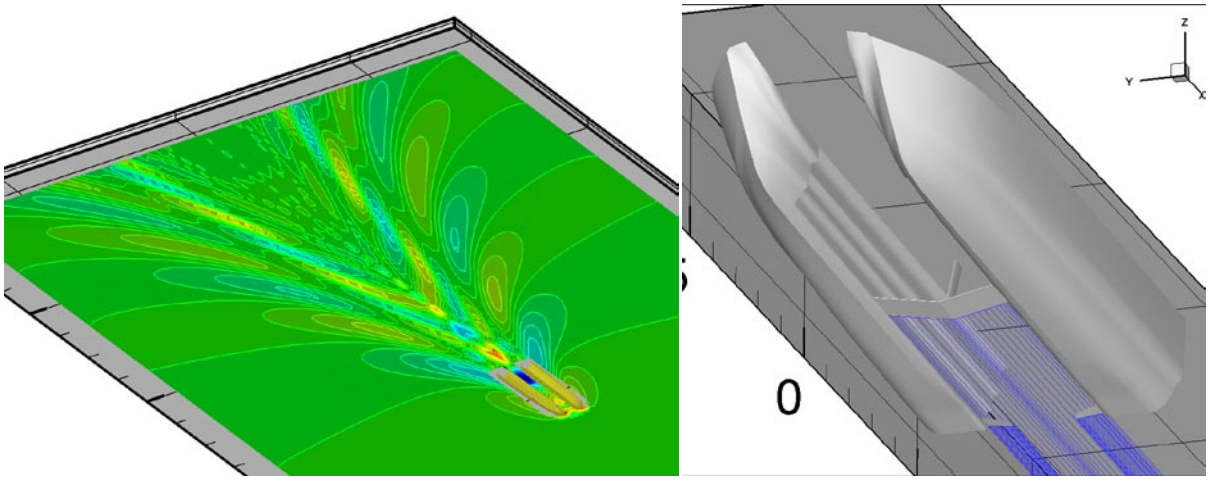

Fig 2: Predicted wave pattern for Fr =0.6 (left) and straight trailing vortices leaving the foils (left).

2. PHASE-A - SENSITIVITY STUDY AND OBJECTIVE FUNCTIONS DEFINITION

Starting from the SPIRIT design, a relatively complex deformation strategy of the hull and foil geometry was defined, and a sensitivity study was produced for the identification of the trends. The general idea is to produce a regular variation of each design parameter at a time, in order to identify useful trends for the new hull. A Free-Form Deformation (FFD) approach was adopted for the parametrical deformation of the hull. The FFD is a technique developed in computer graphics for the animation of objects. The object to be deformed (or a portion of)

is embedded into a box. and then partitioned regularly into a given number of slices with planes orthogonal to one coordinate axis. The vertices of the resulting intersections represent possible control points and their movements are capable of deforming the internal object. Several rules can be adopted in the movements of the control points, e.g. the motion can be inhibited along prescribed directions, or can be linked together with the movement of a different control point.

The FFD box adopted for the bow of the SPIRIT catamaran is illustrated in Fig. 3. Four slices cut the box along the longitudinal axis. The external sections are typically kept fixed (in order to maintain the fairness of the surface at the connections), whenever only a part of the geometry has to be modified. On the selected control points (8 in the picture: 4 on each side of the demihull) a limitation was imposed, allowing only laterally displacements (i.e. along the *y* direction only). Furthermore, all the control points on one side of the hull were linked together: the number of design variables reduced finally to two. A different FFD box was used for the modification of the foil geometry (not reported in the paper), giving two more variables to the problem. Two more variables were added: the longitudinal position of the foil and the demihull spacing. The total number of design variables used for the sensitivity analysis was 6. The effect of the design variables is summarized in table 1.

Table 1: Effect of the variation of the design variables (TE, Trailing Edge; LE, Leading Edge)

Design variable	*Positive values*	*Negative values*
DV1	Enlarge inner bow width	Shrink inner bow width
DV2	Enlarge outer bow width	Shrink outer bow width
DV3	Increase foil thickness – TE	Decrease foil thickness – TE
DV4	Increase foil thickness – LE	Decrease foil thickness – LE
DV5	Foil shifted fore	Foil shifted aft
DV6	Increase demihull spacing	Decrease demihull spacing

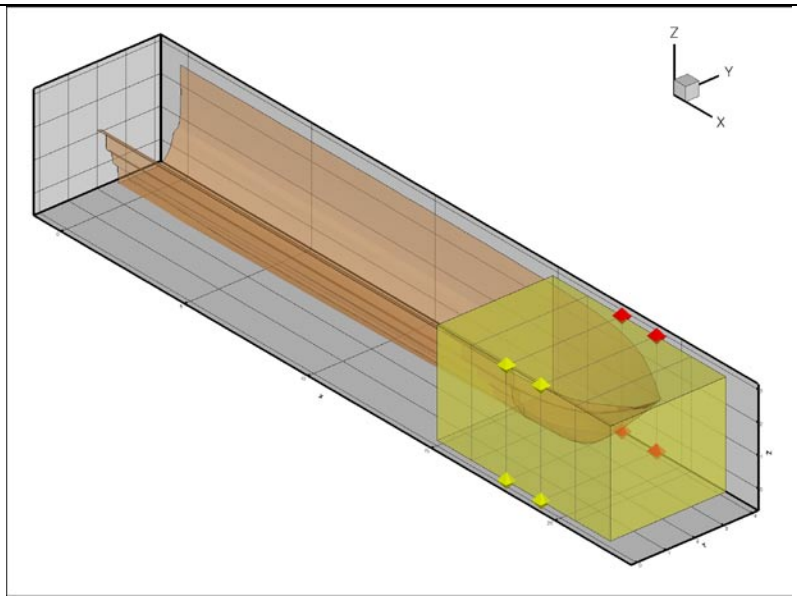

Fig 3: Perspective view of the FFD parameterization. Control points are represented by symbols.

The sensitivity of these variables were computed with respect to the objective functions selected on the base of the analysis of the operative condition of the ship, as discussed together with the designers. The ship is designed to travel at two main speeds (around 18 and 36 knots respectively). Navigation in confined water was performed at the lower speed only, so the wave wash was considered only for this speed. Finally, 3 different objective functions

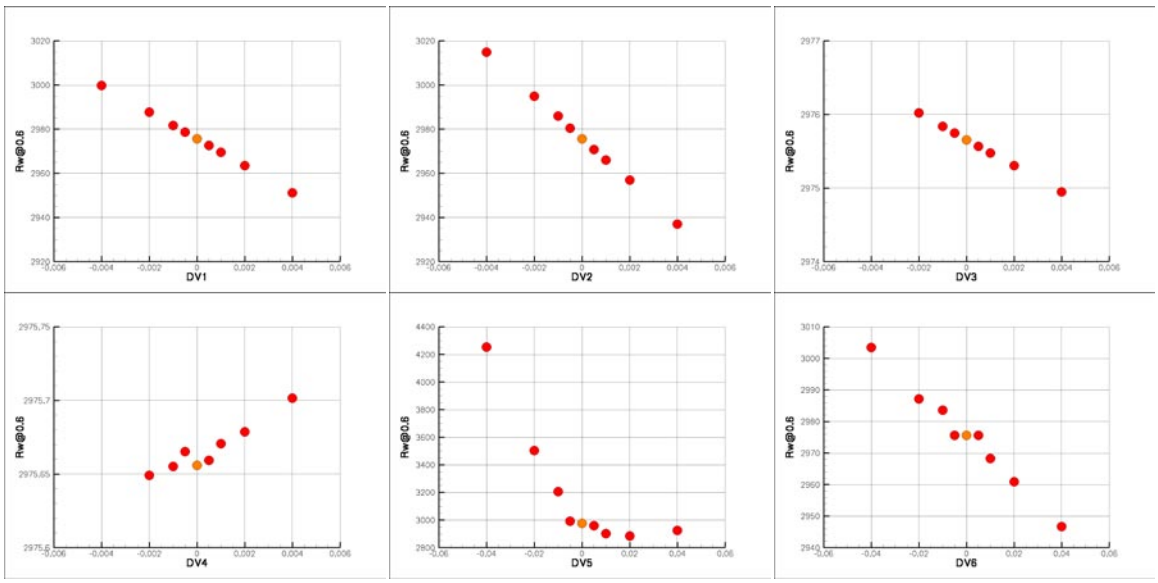

Figure 4: Sensitivity study: trend of the 6 design variables (in abscissa) with respect to the first objective function (wave resistance at Fr=0.6).

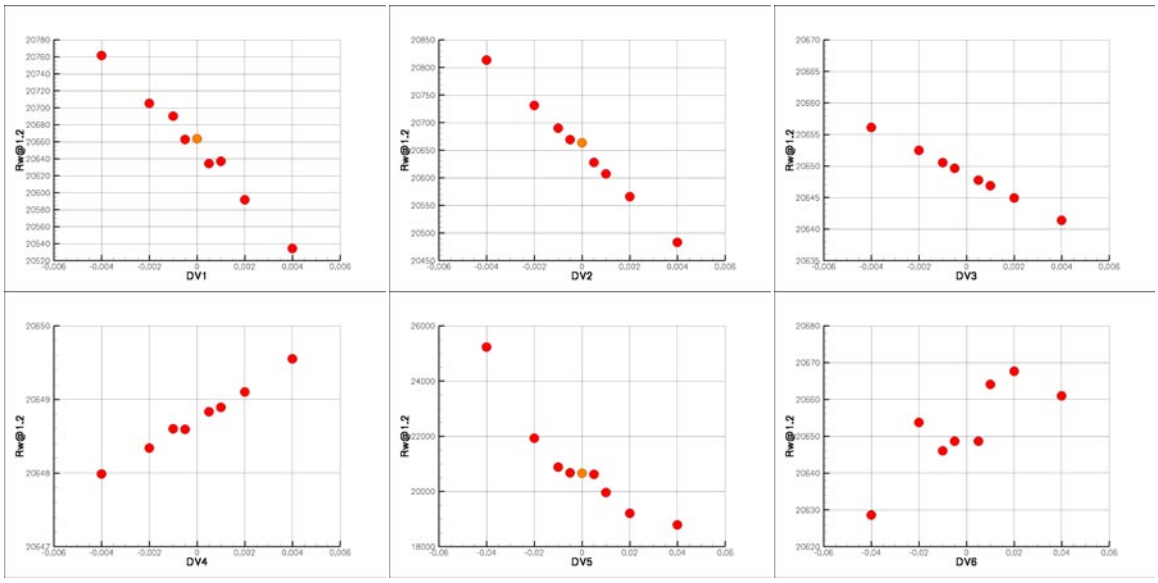

Figure 5: As in Fig. 4, with respect to the second objective function (wave resistance at Fr=1.2).

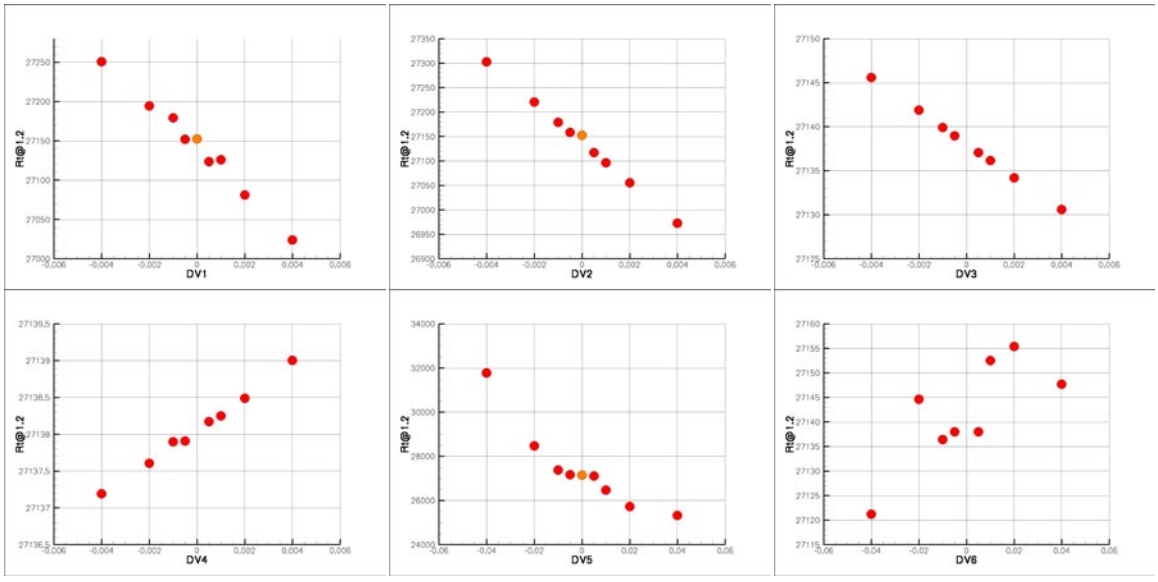

Figure 6: As in Fig. 4, with respect to the third objective function (total resistance at Fr=1.2).

were considered: wave resistance at the two design speeds (Fr=0.6 and Fr=1.2) and total resistance at the higher speed (Fr=1.2). Wave resistance is considered, in a preliminary stage, as representative of associated wave energy, and its minimization is somewhat connected with the reduction of wave wash.

For each design variable by a small perturbation of the hull geometry (changing a single variable at a time). The resulting graphs in Figs 4, 5 and 6 give a visual indication about the trends. Clear tendencies are identified by the sensitivity analysis, at least for the first 5 design variables, whereas DV6 shows opposite trends between objective function 1 and the other two. These information were used by Teknicraft Design Ltd. in the definition of three new designs, selected as the base hulls for the development of the optimal hull shape in PHASE-B.

3. AUTOMATIC GENERATION OF DIFFERENT SHAPES IN PHASE-B

As mentioned before, in *PHASE-B* a morphing technique was applied for the parameterization of the hull and foil geometry. Morphing is commonly adopted in image analysis to derive a new image by using a set of base images. In this particular case, the tentative hull and foil shapes are automatically obtained as a weighted sum of the computational grids produced using three base hulls (say, HULL1, HULL2 and HULL3) and foils (FOIL1, FOIL2 and FOIL3). Once the surface grid has been produced for all the given geometries, using the same number of grid panels and an equivalent grid topology, we have a base for the interpolation. Two variables (HU1 and HU2) are used to combine the shape into the interpolation formula. Once the values for HU1 and HU2 are assigned, three coefficients are defined as follows:

$$c_1 = HU1$$
$$c_2 = (1 - HU1)HU2$$
$$c_3 = (1 - HU1)(1 - HU2)$$

Using these coefficients, the tentative hull is obtained, point by point, by using the following equation, where x_n is the vector of the grid points of the tentative hull in the Cartesian space, and x_1, x_2 and x_3 are the vectors of the grid points of the three base designs in the Cartesian space.

$$x_n = c_1 x_1 + c_2 x_2 + c_3 x_3$$

We recall that, by construction, the following condition holds:

$$c_1 + c_2 + c_3 = 1$$

This approach provide a rationale for mapping the design space onto a unit square, since HU1 and HU2 were varied in between 0 and 1. Necessarily, if HU1 is set to 1 (and hence c_1 =1) all the other coefficients are necessarily zero for any value of HU2.

The same procedure is applied to the foil geometry (FOIL1, FOIL2 and FOIL3 are the conventional names for the base designs) and the design variables are FO1 and FO2. Since the demihull spacing was another design variable, the span of the foil was changed accordingly, filling the gap between the hulls.

4. PROBLEM DEFINITION (PHASE-B)

The three new base designs are reported in Fig 7. The shape of the foils is also reported, showing some differences in the downward angle and in the profile. The three base hulls are combined together by using a morphing technique in order to produce the new hull geometry.

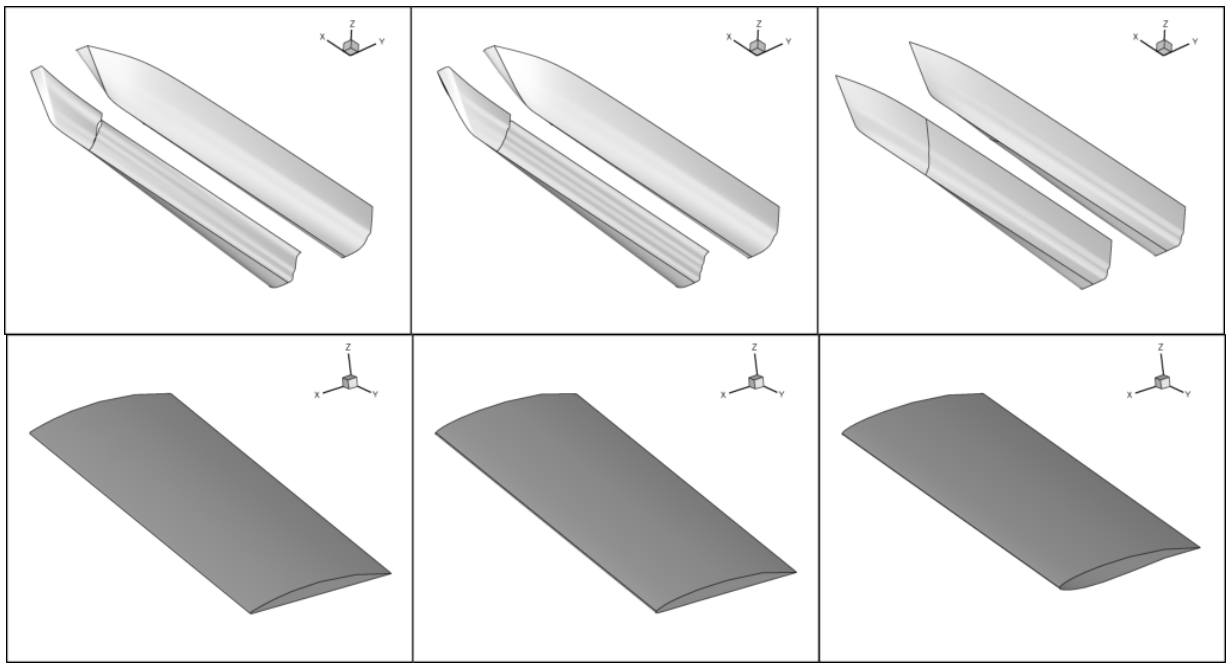

Figure 7: Perspective views of the three initial shapes of the demihulls and of the central foils adopted as a starting point for the design optimization of RV2. A couple of stern flaps as for SPIRIT are also adopted, being the same for all the given configurations (their shape is not reported here).

In *PHASE-B*, we have a different set of design variables. Four of them are represented by the weights for the morphing (two for the hull, two for the foil), while five more variables are also defined, and are reported in table 2. Objective functions are the same already used during the *PHASE-A*. Table 2 reports also the design constraints, who involve box constraints on the displacement and some design variables. A large variation of the displacement is allowed in this phase, in order to completely understand the effect of a strong variation on this parameter.

Table 2. *Description of design variables, constraints and objective functions.*

DESIGN VARIABLES	BOX-CONSTRAINTS	OBJECTIVE FUNCTIONS
Static trim angle (STA)	[-0.3:1.0] deg	Wave resistance at *Fr* = 0.6
Demihull spacing (DSV)	[-2.0:1.0] m	Wave resistance at *Fr* = 1.2
Displacement (DIS)	[72.0:96.0] t	Total resistance at *Fr* = 1.2
Longitudinal Foil Position (LFP)	[-1.0:1.0] m	
Foil Shape Parameter 1 (FO1)	--	
Foil Shape Parameter 2 (FO2)	--	
Hull Shape Parameter 1 (HU1)	--	
Hull Shape Parameter 2 (HU2)	--	
Stern Interceptor Height (SIH)	[0:25] mm	

5. APPROACH FOR THE OPTIMIZATION PROBLEM

The intensive use of high-fidelity, expensive CFD solver inside a SBD is primarily limited by the computational costs. A method to alleviate this problem, is to systematically replace the CFD solver during the optimization phase, by using a fast interpolation model (usually called "*metamodel*") trained on a limited number of expensive simulations, and then monitoring the discrepancies between the high-fidelity solver and the interpolation model. Here, the space design has been initially populated by 64 different configurations, in order to derive the base for the metamodel. In this paper a kriging model (*Matheron 1968, Peri 2009*) was adopted to interpolate the training results. The algorithm here is relatively simple: the optimization process is performed by using the metamodel for the analysis of the ship's performances. Once convergence is obtained, the final shape is validated by the use of the

expensive CFD model. The new computation is then added to the training set to obtain an *improved* metamodel, and the optimization process is repeated until convergence to a final geometry (or the maximum number of iteration) is reached.

To solve the multiobjective problem, the optimization algorithm ***UNICO*** (*Peri and Campana, 2005*) has been applied to approximate the *Pareto* front. It is worthwhile to recall that the *Pareto* front is the set containing the best trade-off solutions computed by the algorithm, i.e. the so-called *non-dominated* solutions (i.e. designs that cannot be improved simultaneously under all the criteria by another solution). Indeed, when we are in presence of more than one single objective function, it is very rare to find one single design able to give the optimal value for all the objective functions at the same time. As a consequence, the designer has to deal with a finite set of configurations containing the best compromise solutions, that is, the *Pareto* set.

In Fig. 8, the history of the 6 design variables values during the entire optimization process is shown. Two different zones are easily noticeable: the first 64 values belong to the training phase. The values of the design variables are assigned according some user-defined sampling technique (we have adopted here a standard *Orthogonal Array* technique), properly selected in order to explore the design space. From configuration number 65 on, the variable values were selected by the *UNICO* optimizer, looking for *Pareto* solutions. Indeed, in Fig. 8 we observe that some of the variables show a precise trend, focusing around some value, whereas for other variables the results appear to be more spread. This because the *Pareto* front can be large over the design variable space. The blue dots represents the values corresponding to designs that were found to be on the *Pareto* front: two *Pareto* solutions were obtained in the training phase whereas the remaining 5 were found by the optimizer. A complete discussion of the *Pareto* front will be given later in the paper.

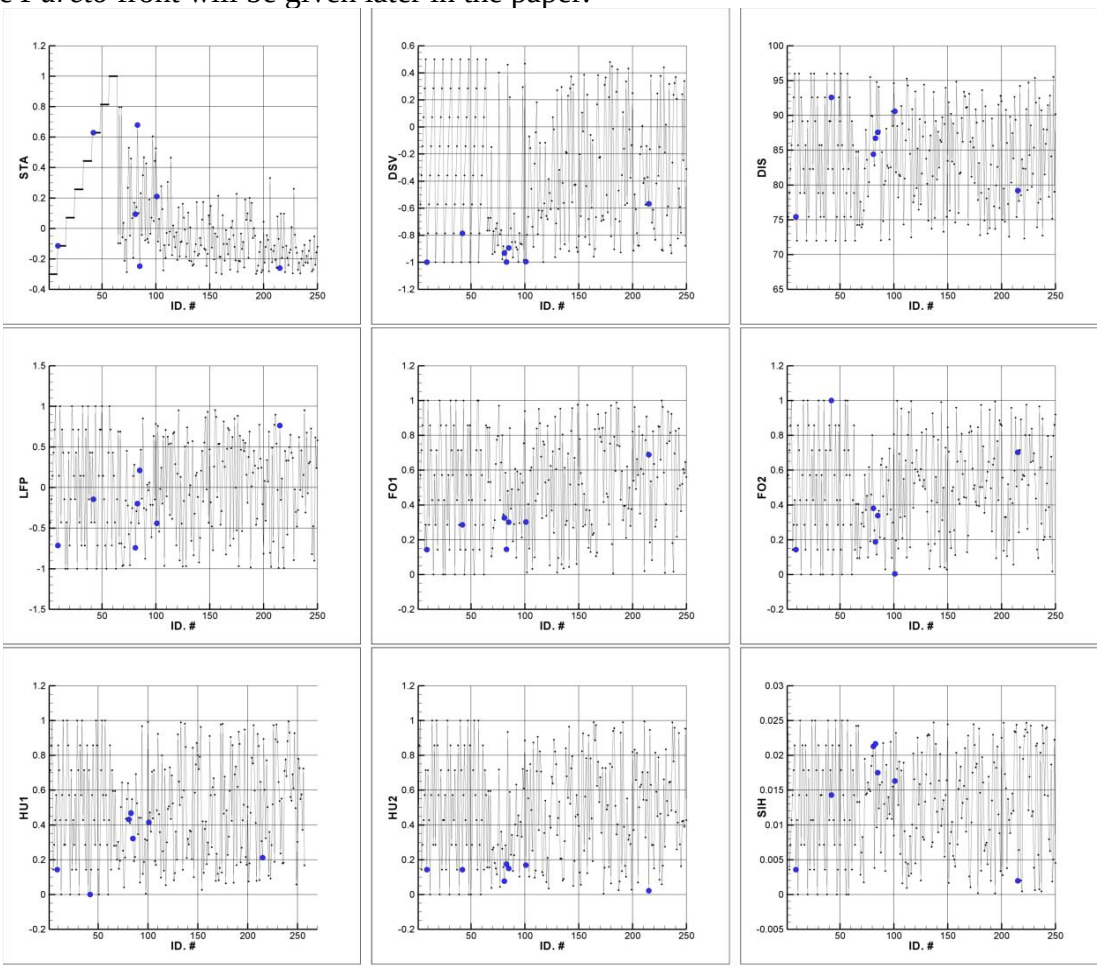

Figure 8: Values of the design variables as a function of the iteration of the optimization algorithm. The blue dots represents the values corresponding to designs that were found to be on the Pareto front.

6. SENSITIVITY ANALYSIS FOR THE FINAL DESIGN

The interpolation of the training data is reported in Fig. 9: each objective function is reported as a function of a single variable while all the others are kept fixed. All the fixed values are the following one:

- STA = 0.35 (i.e. the central value of the range).
- DSV = -0.5 (central value of the range).
- DIS = 84.0 (central value of the range).
- LFP = 0.0 (central value of the range).
- FO1 obtained by setting $c_1 = c_2 = c_3 = 1/3$.
- FO2 obtained by setting $c_1 = c_2 = c_3 = 1/3$.
- HU1 obtained by setting $c_1 = c_2 = c_3 = 1/3$.
- HU2 obtained by setting $c_1 = c_2 = c_3 = 1/3$.
- SIH = 12.5 (central value of the range).

Wave Resistance at Fr=0.6 (F1)

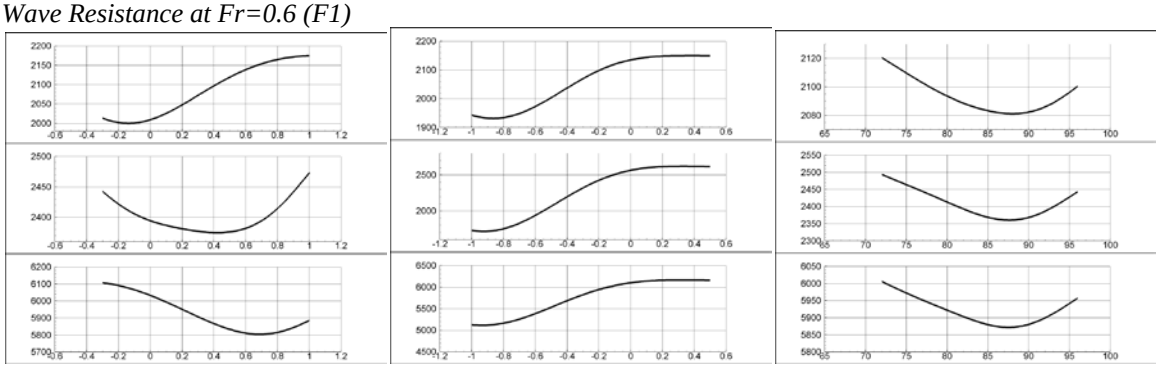

Wave Resistance at Fr=1.2 (F2)

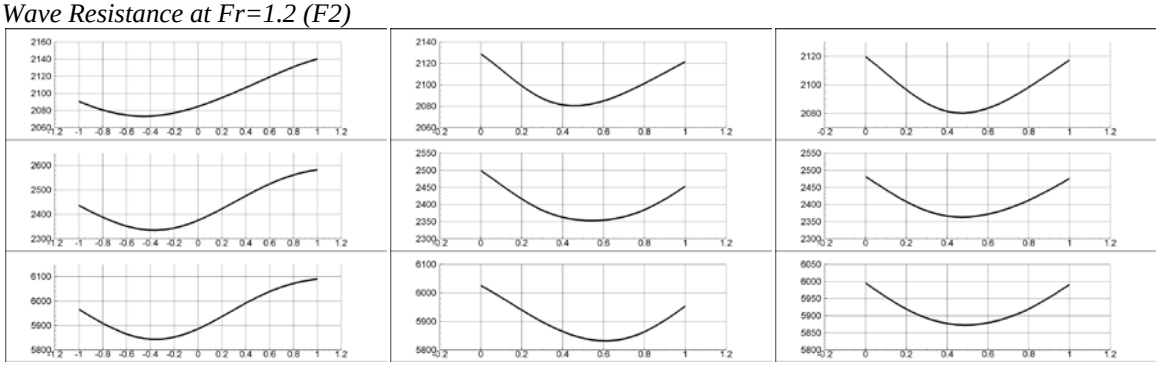

Total Resistance at Fr=1.2 (F3)

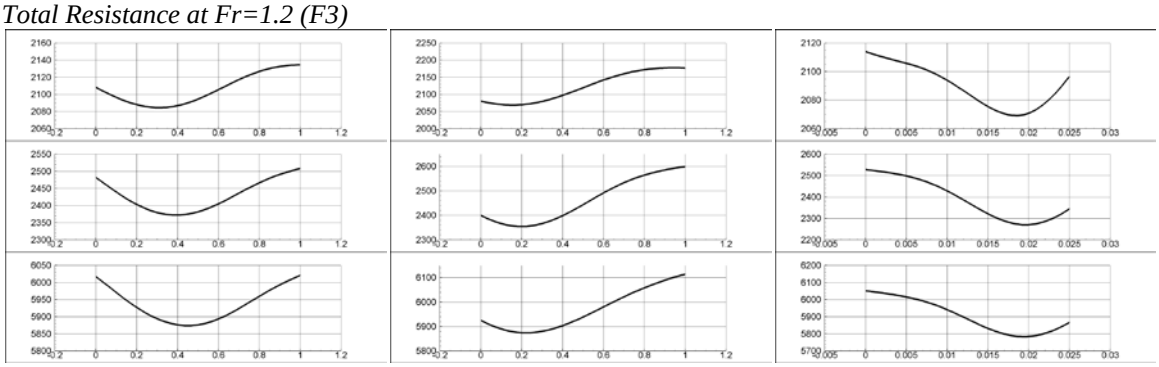

Figure 9: Objective functions cut planes. From top to bottom, the three groups report the wave resistance at Fr=0.6, the wave resistance at Fr=1.2 and the total resistance at Fr=1.2. In each group (from top to bottom, left to right) the plots are for (1)Static Trim Angle, (2)Demihull Spacing Variation, (3)Displacement, (4)Longitudinal Foil Position, (5)Foil Shape Parameter 1, (6)Foil Shape Parameter 2, (7)Hull Shape Parameter 1, (8)Hull Shape Parameter 2, (9)Stern Interceptor Height. Curves are obtained by varying a single parameter at a time around the intermediate hull configuration.

As a consequence, when a minimum is detected on a curve, it is important to remember that the graph is obtained by maintaining all the other design variable fixed at the central value, and all the graphs should be recomputed once one of the design variable value is changed. These pictures are useful because they provide some indications about the descent direction for each single design variable and the order of magnitude of the reduction that a design variable can reasonably produce: in this way, a preference order among the variables can be defined.

Scales for the objective functions are not congruent among the design variable. But is quite evident as the effect on the displacement reduction is very high, obviously. For all the other design variables, the direction of improvement is shared by all the objective functions. The only conflicting behaviour is that of the static trim angle: it shows a contrasting behaviour with respect to the objective functions: a reduction is suggested to improve the first objective function, it is nearly neutral with respect to the second objective function, and an increase is suggested to improve the third objective function. This is a common situation in multiobjective optimization, and it represents always a difficult test in ship design. Numerical multiobjective algorithms are indeed able to provide directly a set of optimal alternatives, reducing the risks of erroneous ranking of one solution with respect to another: the trade-offs are clearly reported, and the designer is put in the condition to clearly understand the benefit of one compromise solution.

7. OPTIMIZATION RESULTS

After the training phase, which evaluated the 64 different configuration uniformly spread in the design space, the real multiobjective problem was tackled. The optimization algorithm ***UNICO*** was applied to identify the *Pareto* front of the problem. The final results are reported in Fig. 10 and in table from 3 to 5.

In Fig. 10, the blue dots are the *Pareto* optimal solutions, while the red circles are all the tested solutions. In table 3 to 5, the value of the objective functions for the *Pareto* solutions are reported. The objective functions are nondimensionalized by the value computed for the original HULL1 hull with the FOIL1 foil.

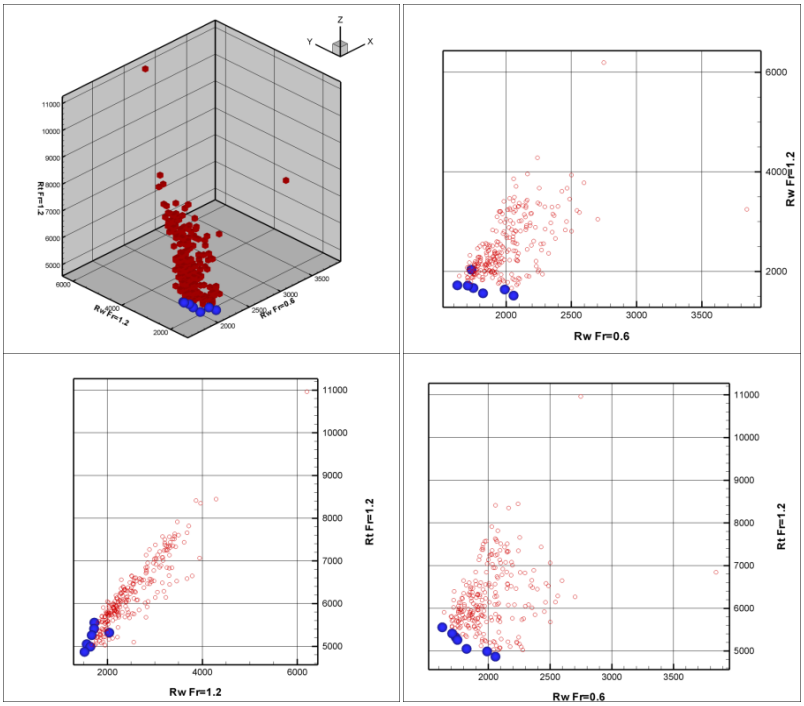

Figure 10: Different views of the resulting Pareto front: from top to bottom, left to right, a perspective view of the Pareto front, and three different views of the Pareto solutions projected onto the planes at constant F1, F2 and F3 values, respectively.

Configuration number #	R_W (Fr=0.6)	R_W (Fr=1.2)	R_T (Fr = 1.2)
9	0.89981	0.85964	0.89463
42	1.04880	0.82049	0.82520
81	0.92221	0.83529	0.86974
83	1.08427	0.75909	0.80506
85	0.85765	0.86244	0.91858
101	0.96110	0.78224	0.83508
215	0.91504	1.01890	0.87966

Table 3: Values of the objective functions for the Pareto designs of the optimization problem.

Configuration number #	C_1	C_2	C_3
9	0.1429	0.1225	0.7347
42	0.0000	0.1429	0.8571
81	0.4324	0.0437	0.5240
83	0.4678	0.0930	0.4392
85	0.3220	0.1018	0.5762
101	0.4147	0.0989	0.4864
215	0.2122	0.0171	0.7707

Table 4: Values of the hull interpolation coefficients for the Pareto designs of the optimization problem.

Configuration number #	C_1	C_2	C_3
9	0.1429	0.1225	0.7347
42	0.2857	0.7143	0.0000
81	0.3259	0.2569	0.4172
83	0.1455	0.1611	0.6934
85	0.3015	0.2369	0.4616
101	0.3024	0.0029	0.6948
215	0.6877	0.2192	0.0931

Table 5: Values of the foil interpolation coefficients for the Pareto designs of the optimization problem.

The solution of the multiobjective problem finally gave the following the following design indications:

Best designs for a single objective: A basic indication for the designer is the best hull each objective function. For F1 (the wave resistance at Fr=0.6) is #85. The best hull for F2 (wave resistance at Fr=1.2) and for F3 (total resistance at Fr=1.2) is #83. However #83 is the worse design for the wave resistance at low speed (F1), a clear indication that that design trend isn't a good trade off.

Trade-off solution (1): In an aggregated approach assuming equal importance (i.e. equal weights) among the three objective functions, the best compromise solution appears to be #101, with an aggregated total value of 0.859 (i.e. an improved performance of -14.1%). Also #81 (0.876) and #85 (0.879) appear to be interesting solutions according to this approach.

Trade-off solution (2): Disregarding completely the lower speed values, the two most interesting design are #83 and #101.

Sensitivity analysis: By looking at Fig. 9 the following indications, with respect to the base design, emerge:

(i) STA needs to be increased for lower speed and decreased for higher speed;
(ii) DSV needs to be decreased;

(iii) LFP needs to be increased;
(iv) FO1 and FO2 needs to be increased;
(v) HU1 and HU2 do not show a clear trend, depending on speed;
(vi) SIH needs to be increased;

Design variable analysis: Finally, by looking at Fig. 8 other suggestions came too:

(i) only DSV, FO1 and HU2 produce a clear trends, all of them showing better performances for low values;
(ii) all the other design variables show unclear trends with the speed.

In Fig. 11, a view of the hull #101 with a zoom of its foil is reported. The sensitivity analysis around this configuration is plotted in Fig. 12, based on the *kriging* estimates. The plot highlights the presence of a stationary point with respect to all the design variables and objective function, confirming the good qualities of the selected hull and indirectly demonstrating the validity of the optimization process: in fact, appears clearly that the present configuration cannot be improved by a small variation of the design variables, so that the optimizer identified a local optimum point.

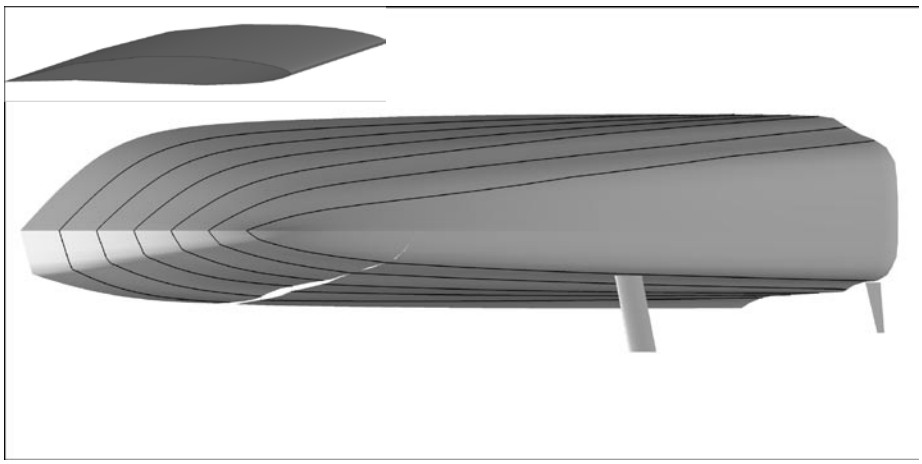

Figure 11: Perspective view of configuration number 101 and of the corresponding foil.

Wave Resistance at Fr=0.6 (F1)

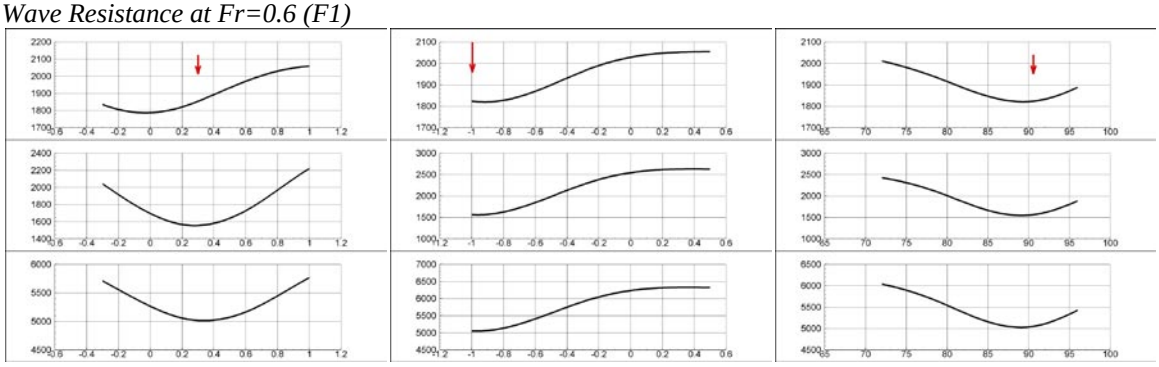

Wave Resistance at Fr=1.2 (F2)

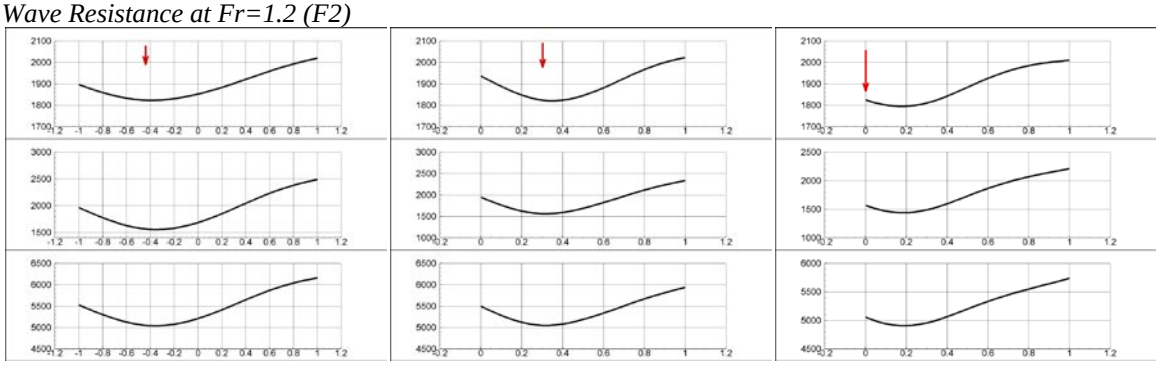

Total Resistance at Fr=1.2 (F3)

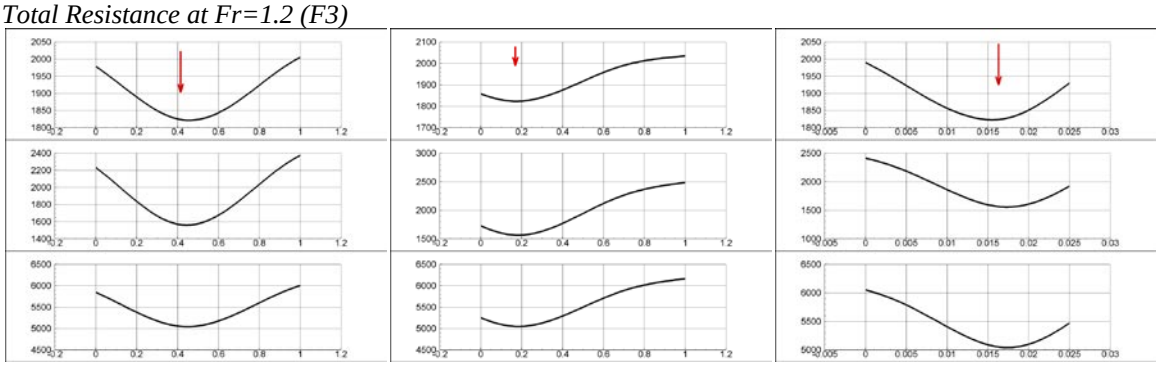

Figure 12: Objective functions cut planes. From top to bottom, the three groups report the wave resistance at Fr=0.6, the wave resistance at Fr=1.2 and the total resistance at Fr=1.2. In each group (from top to bottom, left to right) the plots are for (1)Static Trim Angle, (2)Demihull Spacing Variation, (3)Displacement, (4)Longitudinal Foil Position, (5)Foil Shape Parameter 1, (6)Foil Shape Parameter 2, (7)Hull Shape Parameter 1, (8)Hull Shape Parameter 2, (9)Stern Interceptor Height. Curves are obtained by varying a single parameter at a time around the hull configuration number 101. The arrow gives the position of the optimal value for each parameter.

ACKNOWLEDGMENTS

This research is sponsored by Pacific International Engineering PLLC contract # KT-05-343 under the administration of Dr. Philip D. Osborne.

REFERENCES

Bassanini, P., Bulgarelli, U., Campana, E.F., Lalli, F., *The Wave Resistance Problem in a Boundary Integral Formulation*, **Surveys on Mathematics for Industry**, 1994, 4: 151-194

Bollay W (1936), *A new theory for wings of small aspect ratio*, **PhD thesis**, California Inst. Of Technology

Campana, E F., Liuzzi, G., Lucidi, S., Peri, D., Piccialli, V., Pinto, A., New global optimization methods for ship design problems, **Optimization and Engineering**, in press, 2009.

Landrini M, Campana EF (1996), *Steady Waves and Forces About a Yawing Flat Plate*, **J. Ship Research**, Vol.40(3).

Matheron, G. (1963), *Principles of geostatistics*, **Economic Geology**, **58**, pp. 1246-1266.

Peri D, Campana EF (2005), *High-Fidelity Models in Global Optimization*, **Lecture Notes in Computer Science,** 3478, pp. 112-126.

Peri D, (2009), *Self-Learning Metamodels for Optimization*. **Ship Technology Research**, Vol 56, pp. 94-108.

Pinto A., Peri, D., Campana,E.F., *Multiobjective Optimization of a Containership using Deterministic Particle Swarm Optimization*, **Journal of Ship Research,** Vol.51(3), 217-228, 2007.

Osborne PD, Côté JM, MacDonald N, de Waal N, (2009), *Full-scale measurements and impact studies with high speed foil-assisted catamarans in a wake sensitive area*, **10th Int. Conf. on Fast Sea Transportation, FAST 2009**, Athens, Greece.